Supporting Information

Reversible Magnesium Intercalation into a Layered Oxyfluoride Cathode

Jared T. Incorvati,[1,4] Liwen F. Wan,[2,4] Baris Key,[3,4] Dehua Zhou,[3] Chen Liao,[3,4] Lindsay Fuoco,[1,4] Michael Holland,[1] Hao Wang,[3,4] David Prendergast,[2,4] Kenneth R. Poeppelmeier,[1,3,4] John T. Vaughey[3,4,*]

[1] Department of Chemistry, Northwestern University, Evanston, Illinois, 60208, United States

[2] The Molecular Foundry, Lawrence Berkeley National Laboratory, Berkeley, CA 94720 United States

[3]Chemical Sciences and Engineering, Argonne National Laboratory, Lemont, Illinois, 60439, United States

[4]The Joint Center for Energy Storage Research

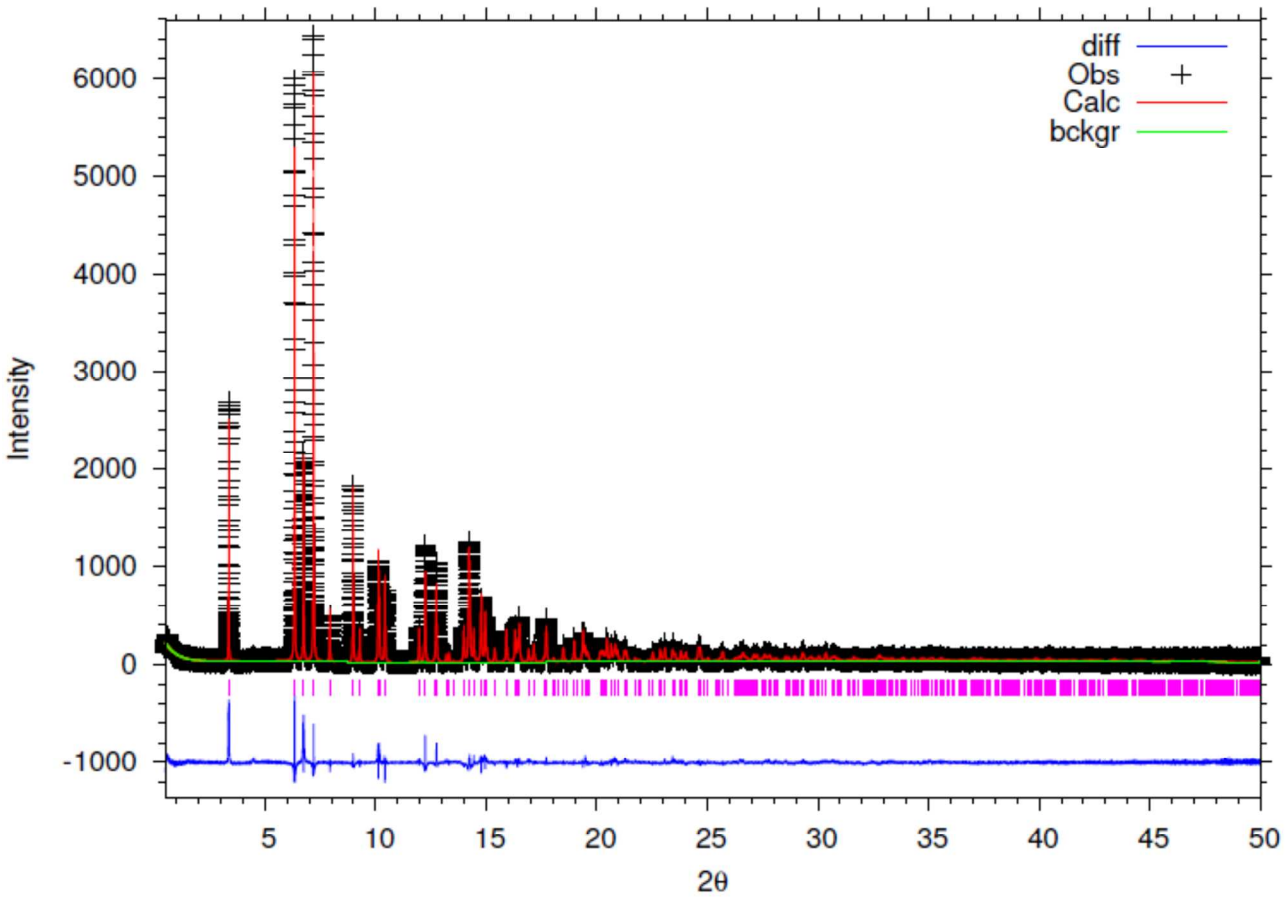

Figure S1. Rietveld refined PXRD data of $MoO_{2.8}F_{0.2}$ showing experimental, calculated, and difference, patterns along with Bragg reflections (Pink).

Rietveld Refinement. Rietveld refinement of the synthesized $MoO_{2.8}F_{0.2}$ was carried out using the GSAS package against literature crystal data[1] for $MoO_{2.8}F_{0.2}$ with space group Cmcm(63) . Data was collected on 11-bm of the Advanced Photon Source at Argonne National Laboratory.

Synthesis. Caution is required when handling hydrofluoric acid as it is toxic and corrosive. Appropriate personal protective equipment and training are required.

$MoO_{2.8}F_{0.2}$ was synthesized from molybdenum trioxide (α-MoO_3, 99.5%), molybdenum metal (Mo), and hydrofluoric acid ($HF_{(aq)}$, 48% w/w in water) that were obtained from Sigma Aldrich and were used as received. In a representative synthesis, α-MoO_3 powder (4.8g, 33mmol) was combined with Mo powder (120mg, 1.25mmol). The dry reagents were mixed thoroughly and combined with DI water (37.5mL) and 48% $HF_{(aq)}$ (12.5mL, 334mmol) in a Teflon liner from a 125mL autoclave from Parr. The autoclave was heated to 240°C and held for 24 hours. The contents of the autoclave were vacuum filtered, washed with DI water, and allowed to dry in air. The synthesis yielded 1.7 grams of dark blue powder, a ~35% yield based on α-MoO_3. Synthetically, the system tolerates a modest excess of α-MoO_3, which will remain in solution upon cooling, however excess Mo results in isolation of a more reduced cubic phase, $MoO_{2.6}F_{0.4}$, with a structure related to ReO_3. Extensive mixing of the solid reagents before the reaction is critical to produce a phase-pure product.

Extensive mixing of solids is critical to formation a phase-pure product. Mixing was achieved at a 5g scale by combining solids in a 10ml plastic test tube, sealing, and shaking for 2 minutes. Smaller scale reactions could readily be mixed by grinding in a mortar and pestle.

Particle size is quite large for use in a device. Grinding in a ball mill reduces most particles to roughly micron size, but some nearly full sized plates remain. This is in good agreement with preferred orientation observed in PXRD of the laminate.

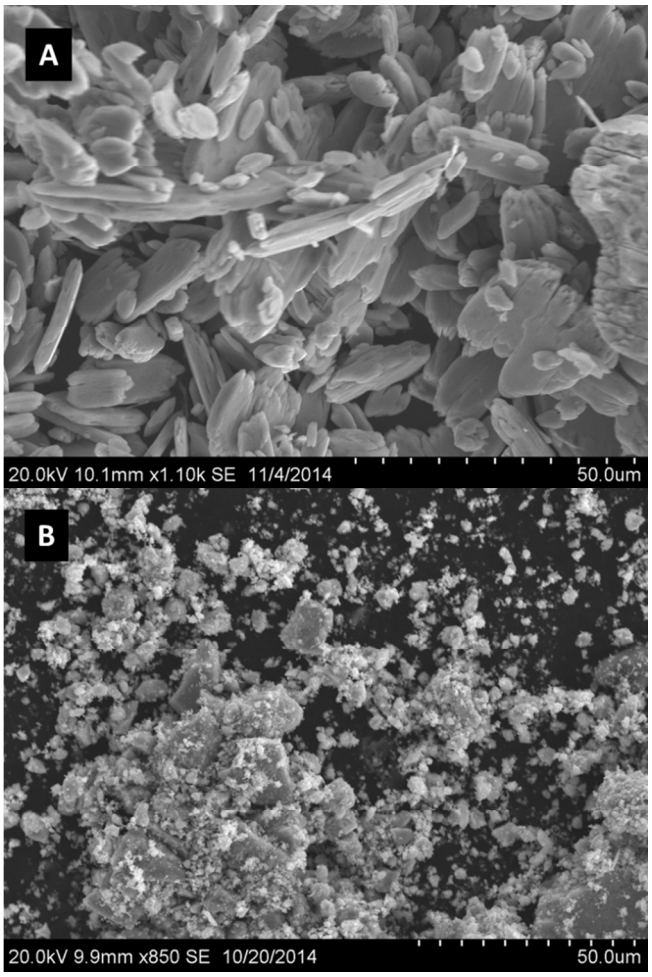

Figure S2. SEM images of A) $MoO_{2.8}F_{0.2}$ product particles, and B) $MoO_{2.8}F_{0.2}$ particles after 20 minutes of ball milling for use in laminate making and cell construction.

Elemental Analysis. Elemental analysis was carried out by Galbraith Laboratories Inc. which performed ICP to determine molybdenum content and Pyrohydrolysis to determine fluorine content. Analysis revealed that the samples synthesized and used in this paper contained 2.70% F and 62.8% Mo corresponding to a molar ratio of .217 moles of F per mole of Mo.

The formula $MoO_{2.8}F_{0.2}$ is used throughout the text for simplicity.

Cathode and Cell Construction. Cathodes were prepared from $MoO_{2.8}F_{0.2}$ by grinding the material in a ball mill and preparing a slurry of the active material, with acetylene black, and poly(vinylidene difluoride) (PVdF) in the ratio 80:10:10 while suspended in *N*-methylpyrrolidone (NMP). The slurry was then cast as a 200 micron thick film on a sheet of stainless steel foil and dried in an oven at 70°C for 4 hours. Individual 0.97cm^2 cathodes were punched from the foil to be electrochemically evaluated in 2032 coin cells. α-MoO_3 cathodes were prepared analogously. A bistriflimide, or TFSI, electrolyte was used consisting of 0.2M $Mg(TFSI)_2$ in propylene carbonate (PC), and a high surface area carbon supercapacitor-type BP-2000 carbon black cast on stainless steel was the counter electrode.[2] In a typical experiment, coin cells were cycled on a Maccor battery cycler at a current of 5μA between voltages of -1.5 to 1.5V.

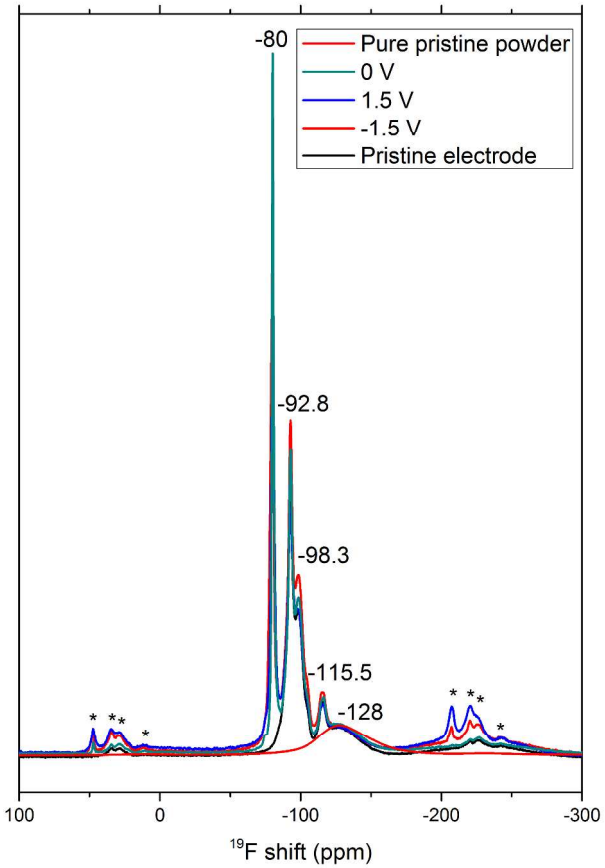

Figure S3. The ^{19}F MAS NMR spectra of pristine oxyfluoride powder, electrode and electrochemically cycled $Mg_{x}MoO_{2.8}F_{0.2}$ samples collected (discharged to 0V, -1.5V and charged to 1.5V) at 11.7 T. Signal is in reference to $CFCl_3$ at zero ppm and a recycle delay of 2s is used. Spinning speed of 60kHz are used. -80 ppm is due to residual $Mg(TFSI)_2$. -92.8, -98.3 and -115.5ppm resonances are due to PVDF in the electrode mixture. -128 ppm is due to lattice fluorine and remains unchanged upon cycling (single site, ascribed to O_2 sites). No MgF_2 formation is observed which resonates at -197ppm. The spectra intensities are not normalized. * indicates spinning sidebands.

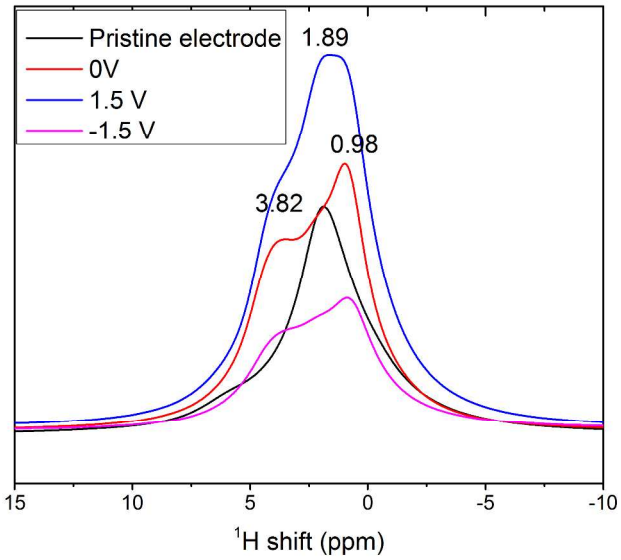

Figure S4. The ^{1}H MAS NMR spectra of pristine oxyfluoride powder, electrode and electrochemically cycled $Mg_{x}MoO_{2.8}F_{0.2}$ samples collected (discharged to 0V, -1.5V and charged to 1.5V) at 7.02 T. Signal is in reference to TMS at zero ppm and a recycle delay of 2s is used. Spinning speed of 60kHz are used. 3.82 ppm and 0.98ppm are due to residual adsorbed PC. 1.89 ppm is tentatively assigned to lattice protons (-OH termination) in the sample which remains largely unchanged upon cycling.

Calculation Methods. The structural optimization and electronic calculations are carried out using the Vienna Ab initio Simulation Package (VASP)[3] that uses planewaves to represent the electronic wavefunctions and the projector-augmented-wave (PAW) method[4, 5] to approximate the electron-ion interactions. Note that standard DFT techniques, such as LDA and GGA, lack electronic descriptions of non-local London dispersion forces that are essential to capture the long-range attractive forces between the double-layers in α-MoO_3. In this work, we use the optB86b-vdW functional,[6] which optimizes the exchange energy in DFT to accurately predict the vdW gap as shown in Table 2. In addition, an on-site Hubbard U term is further added to Mo d-states based on the optB86b-vdW optimized crystal structure. This U term is particularly important for investigating the defect states induced by the interactions between Mo and other impurity atoms, such as magnesium and fluorine, and the predictions of formation energies associated with these defects, such as the magnesium intercalation voltage and fluorine substitution energy. In this work, we use U = 4.0 eV, a value that is chosen to reproduce the Mg intercalation voltage for pristine α-MoO_3.

Table 1: Relative formation energies for fluorine substitution with the reference O2 substitution as the lowest energy configuration.

Equivalent oxygen site	ΔE_F (optB86b-vdW)	ΔE_F (optB86b-vdW+U)
O_1	0.65 eV	0.55 eV
O_2	0 (Ref.)	0 (Ref.)
O_3	1.03 eV	1.31 eV

Table 2: Calculated structural parameters for pristine α-MoO_3 using different DFT functionals and compared with experiment.[7]

Method	Lattice constant			vdW gap (Å)	Mo-O_1 bond length (Å)	Mo-O_2 bond length (Å)	Mo-O_3 bond length (Å)
	a (Å)	b (Å)	c (Å)				
PBE	3.97	14.93	3.72	1.13	1.70	1.77 & 2.23	1.96 & 2.43
optB86b-vdW	3.93	13.94	3.72	0.68	1.70	1.77 & 2.18	1.96 & 2.39
Exp.	3.96	13.86	3.70	0.80	1.66	1.73 & 2.25	1.95 & 2.34

References

(1) Pierce, J. W.; Vlasse, M., The crystal structures of two oxyfluorides of molybdenum. *Acta Crystallogr., Sect. B: Struct. Sci., Cryst. Eng. Mater.* **1971,** 27, 158-163.

(2) Amatucci, G. G.; Badway, F.; Du Pasquier, A.; Zheng, T., An Asymmetric Hybrid Nonaqueous Energy Storage Cell. *J. Electrochem. Soc.* **2001,** 148, A930-A939.

(3) Kresse, G.; Furthmüller, J., Efficiency of ab-initio total energy calculations for metals and semiconductors using a plane-wave basis set. *Comput. Mater. Sci.* **1996,** 6, 15-50.

(4) Blöchl, P. E., Projector augmented-wave method. *Phys. Rev. B: Condens. Matter Mater. Phys.* **1994,** 50, 17953-17979.

(5) Kresse, G.; Joubert, D., From ultrasoft pseudopotentials to the projector augmented-wave method. *Phys. Rev. B: Condens. Matter Mater. Phys.* **1999,** 59, 1758-1775.

(6) Jiří, K.; David, R. B.; Angelos, M., Chemical accuracy for the van der Waals density functional. *J. Phys.: Condens. Matter* **2010,** 22, 022201.

(7) Kihlborg, L., Least-Squares Refinement of the Crystal Structure of Mo Trioxide. *Ark. Kemi* **1963,** 21, 357-64.